Check for updates

Stimuli-responsive thiocarbamate-based polymeric particles for hydrogen sulfide generation†

Daniel A. Paterson, Aggie Lawer, [ID] Jared Davidson, Sarah Hook and Allan B. Gamble [ID] *

Hydrogen sulfide (H_2S) imbalance has been implicated in pathologies, and reinstating H_2S homeostasis could be a useful therapeutic strategy. However, delivery of H_2S to the disease site remains a challenge. Functionalised nanoformulations could be used as a strategy to deliver high concentrations of H_2S in a targeted manner. Use of a disease-associated trigger that activates and releases H_2S would provide therapeutic selectivity. As proof-of-concept, synthesis and formulation of block co-polymers bearing a thiocarbamate bond, a carbonyl sulfide (COS) precursor, is described. Activation by hydrogen peroxide (H_2O_2), and a subsequent 1,6-self-immolation process leads to release of COS, which in the presence of carbonic anhydrase is hydrolysed to H_2S. H_2S generation was exemplified by reduction of an azido-profluorophore. Formulation of the polymer resulted in compound vesicles that were able to encapsulate a model drug and could be useful in future biological studies exploring delivery of H_2S as a therapeutic, or to activate azido-masked prodrug/pro-fluorophore in areas of high reactive oxygen species (ROS).

Introduction

Hydrogen sulfide (H_2S) is a gaseous cell signalling molecule[1] that is essential in maintaining homeostasis.[2–4] Low levels of H_2S are associated with, but not limited to, neurodegenerative disease (*e.g.*, Alzheimer's disease),[5] cardiovascular disease (*e.g.*, myocardial infarction),[6,7] pain[2] and liver disease (*e.g.*, non-alcoholic Steatohepatitis).[8] Abnormal or unregulated levels of H_2S have been linked to cancer.[9,10] The loss of antioxidant effects when H_2S homeostasis is not maintained is thought to play a key role in disease progression,[11] hence therapeutics that can deliver H_2S (H_2S-donors) are of great interest.[12,13] H_2S, being a noxious gas, is delivered as a precursor, generally in the form of a salt (NaSH or Na_2S) or small molecule (*e.g.*, AP39 [1,2-dithiolethione][14] or GYY4137 [modified Lawesson's reagent][15]). There are limitations in using salt-based H_2S-donors, including rapid hydrolysis in water and an uncontrolled burst release.[16] Non-specific, slow-releasing H_2S-donors and rapid triggerable H_2S-donors that can be activated by a non-specific stimuli (*e.g.*, AP39 hydrolysis[14]), or specific endogenous stimuli (*e.g.*, cysteine-sensitive dithioesters[17] and self-amplifying H_2S azide capped thiocarbamates[17,18]) have

School of Pharmacy, University of Otago, 18 Frederick St, Dunedin, New Zealand, 9054. E-mail: allan.gamble@otago.ac.nz

been documented. However, the concentration of H_2S that can be generated *in situ* is limited for small molecules,[19] and careful consideration of the pharmacokinetics and distribution profiles in designing small molecule H_2S-donors is required.[13]

H_2S delivered in particulate systems, such as liposomes and polymeric particles (*e.g.*, micelles, polymersomes and bicontinuous nanospheres), could improve delivery. Particles could enable prolonged release and increased local levels of H_2S as well as improving stability and aqueous solubility of the H_2S-donor.[20] In addition to the delivery of a H_2S payload, particles could co-deliver a second payload, for example a drug or diagnostic cargo,[21,22] to gain synergistic benefits. Due to polymers versatility, polymeric particles are of great interest in stimuli-responsive drug delivery and more recently H_2S generation.[18,23,24] The amphiphilic block co-polymers (BCPs) that form particles in solution are synthetically adaptable and enable a precursory H_2S-donor to be built-in to the hydrophobic polymer backbone.[17,20,23] Upon formulation, any cargo is protected from the environment, and in the case of H_2S donors,[20,24,25] the stimuli-responsive/triggerable H_2S precursor functional group is protected in the hydrophobic part of the particle.

Much like small molecule prodrugs[26,27] and H_2S-donors,[14,20] the stimulus for particle activation can be endogenous to the disease (*e.g.*, reactive oxygen species [ROS]) or exogenous (*e.g.*, light-activation). Recent examples of stimuli-responsive H_2S-donor particles include those that have

used the *S*-aroylthiooxime (SATO) group and perthiols.[24,28] However, there are no reports of the *p*-aminobenzyloxycarbonyl (PABC) and *p*-hydroxybenzyloxycarbonyl (PHBC) self-immolative linkers, commonly used in prodrug strategies, in H$_2$S-donor particles. Due to the ease in which the stimuli-responsive trigger group on the PABC/PHBC linker can be modified to suit the disease-associated stimulus, we designed a BCP that contains a thiocarbamate group as part of an arylboronate self-immolative linker (*p*-boronate-benzyloxythiocarbonyl; BBOT), using existing aryl boronate trigger moieties linked with methacrylates to form novel BCPs. Combined with a hydrophilic PEG unit, the synthesised BCP can be readily formulated into particles that are responsive to hydrogen peroxide (H$_2$O$_2$),[29–31] a ROS produced by the immune system in response to various pathological conditions (Fig. 1).

Herein, we report on the synthesis of stimuli-responsive PEG-BBOT polymers and explore their H$_2$S-producing capabilities in polymer and particle form (compound vesicles). The production of H$_2$S *via* carbonic anhydrase-catalysed hydrolysis of carbonyl sulfide (COS) is exemplified by activation of an azido-functionalised pro-fluorescent dye. The particles show potential to generate high local concentrations of H$_2$S for activation of azido-functionalised prodrugs or probes (Fig. 1).

Results and discussion
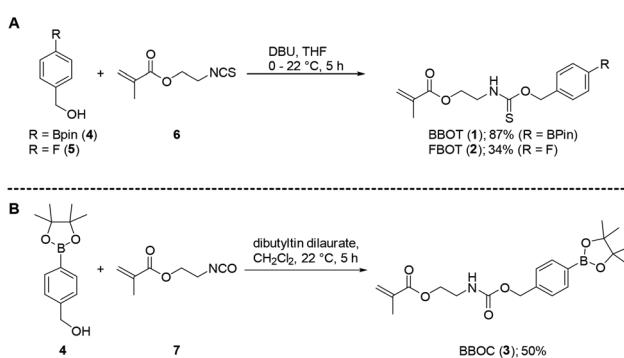
Synthesis of thiocarbamate and carbamate methacrylates

Small molecule and macromolecular H$_2$S-donors normally lead to the direct generation of H$_2$S,[9] with mechanisms that fall into the following classes: (i) hydrolysis-mediated, (ii) thiol-promoted, (iii) photoactivation-mediated or enzyme-mediated.[32] More recently, the generation of H$_2$S *via* carbonic anhydrase-mediated hydrolysis of carbonyl sulfide (COS)[33] has been gaining traction in H$_2$S-donor research, with the ubiquitous carbonic anhydrase facilitating COS hydrolysis at the site of COS release. The precursor to COS is a thiocarbamate bond which is easily incorporated into PABC/PHBC-type self-immolative linkers.[34] The use of a self-immolative linker as a COS donor provides an immediate advantage over other H$_2$S generation methods as simple modification of the linker can enable the user to select the stimulus required for activation of

COS/H$_2$S. Pluth and co-workers have reported on the activation of self-immolative linkers that generate COS/H$_2$S,[34] using stimuli such as H$_2$O$_2$.[35–37] The synthetic flexibility of the self-immolative linkers and responsive capping groups facilitates their incorporation into macromolecules as hydrophobic segments of BCPs.

Herein, COS-releasing *p*-boronate-benzyloxythiocarbamate (BBOT, **1**) was prepared by reacting 4-(hydroxymethyl)phenylboronic acid pinacol ester **4** with 2-isothiocyanatoethyl methacrylate **6** (Scheme 1A). As a control, a non-ROS-responsive *p*-fluoro-benzyloxythiocarbamate (FBOT, **2**) was prepared from the reaction of benzyl alcohol **5** with isothiocyanate **6** (Scheme 1A) and a CO$_2$-releasing carbamate methacrylate *p*-boronate-benzyloxycarbamate (BBOC, **3**) was synthesised by reacting benzyl alcohol **4** with isocyanate **7** (Scheme 1B).[38,39]

Prior to polymerisation with mPEG, the stimuli-responsiveness of methacrylates **1–3** to an oxidant (H$_2$O$_2$) (Scheme 2) was examined. Previous thiocarbamate-based COS-donors have used anilines as the leaving group,[18,37] but in this instance an alkyl amine is released from the BBOT monomers after oxidatively driven self-immolation. Excess H$_2$O$_2$ was added to BBOT (**1**), FBOT (**2**) and BBOC (**3**), with the oxidation and self-immolation progress monitored by ^{1}H NMR spectroscopy (Scheme 2, Fig. 2 [BBOT], Fig. S1 [FBOT] and S2/S3 [BBOC]†). Exposure of the FBOT control polymer to H$_2$O$_2$ resulted in no change to the ^{1}H NMR (Fig. S1†). This suggests that the other functional

Scheme 1 Synthesis of self-immolative (A) thiocarbamate and (B) carbamate methacrylate monomers.
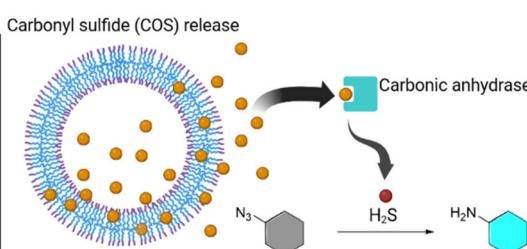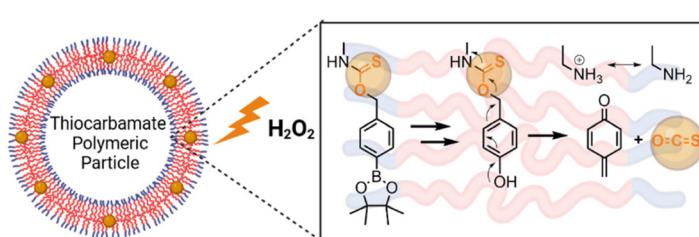
**Fig. 1** Proposed activation and release of carbonyl sulfide (COS) from thiocarbamate-modified polymeric nanoparticles *via* a hydrogen peroxide (H$_2$O$_2$)-triggered arylboronate oxidation and self-immolation. COS is catalytically and rapidly hydrolysed to hydrogen sulfide (H$_2$S) by carbonic anhydrase. The H$_2$S generated by the particles has potential as a direct H$_2$S therapeutic or in the reductive activation of diagnostic or therapeutic aryl azides (*i.e.*, pro-fluorophores and prodrugs). Created in BioRender. Gamble, A. (2025) https://BioRender.com/a62d458.

© 2025 The Author(s). Published by the Royal Society of Chemistry

RSC Appl. Polym., 2025, **3**, 926–933 | **927**
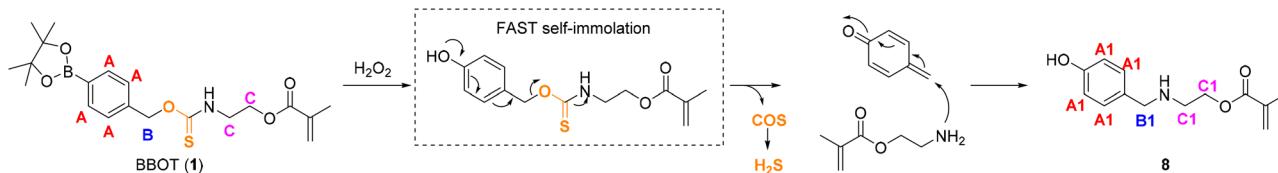
Scheme 2 Oxidation of arylboronate thiocarbamate monomer (BBOT; **1**) with H_2O_2 and proposed trapping of methide observed using ^{1}H NMR spectroscopy.
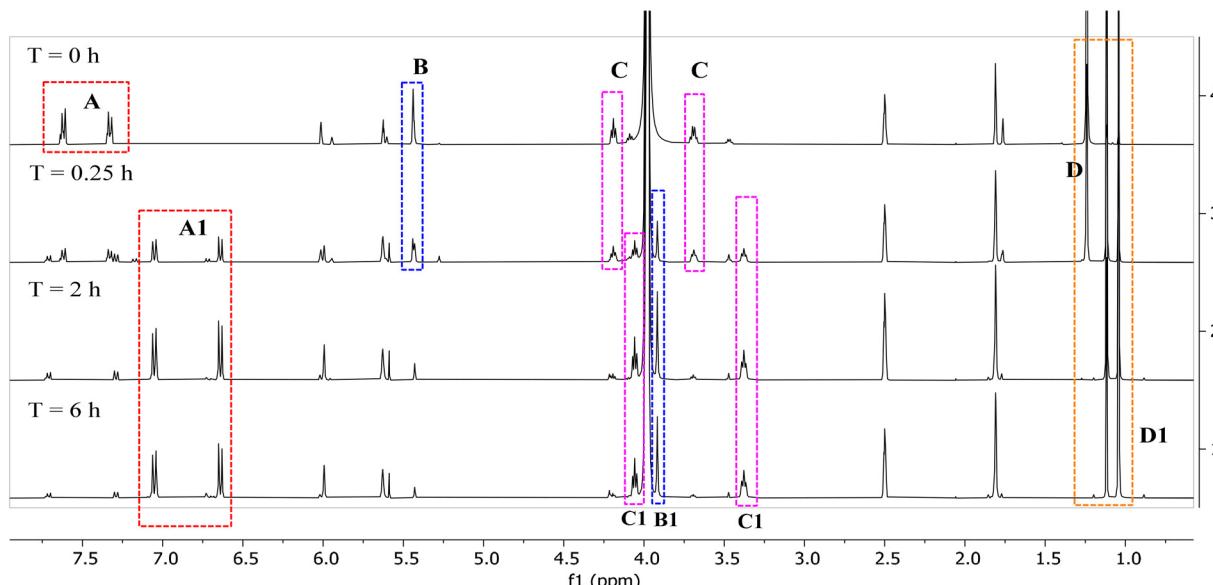

Fig. 2 ^{1}H NMR of BBOT monomer (**1**) at 0, 0.25, 2 and 6 hours post-exposure to excess H_2O_2 in DMSO-d_6:D_2O-PBS solution (25 °C). The key changes in chemical shift that indicate rapid oxidation to the phenol and subsequent self-immolation are annotated as A to A1, B to B1, C to C1 (refer to Scheme 2) and D to D1 (pinacol protons). In BBOT (**1**) (top spectrum) the thiocarbamate bond gives rise to rotamers.[40]

groups in the monomers are stable towards H_2O_2, and the response observed in BBOT (**1**) can be attributed to boronic ester oxidation.

The initial oxidation of the arylboronate BBOT (**1**) (Scheme 2) to the corresponding phenol and free pinacol boronic ester was confirmed by an upfield shift in the aromatic proton resonances (Fig. 2, peaks A to A1). Small amounts of arylboronic ester hydrolysis to the arylboronic acid was observed in the aromatic region (minor peaks at δ 7.25 to 7.75 ppm), and the upfield shift of the pinacol protons (peak D to D1) indicated hydrolysis of the released pinacol boronate ester (after phenol formation) to orthoboric acid and 2,3-dimethylbutane-2,3-diol. The oxidation step for **1** was comparable to that of the control BBOC monomer **3**, which was transformed to the phenol within 2 hours (Fig. S2,† peak A to A1).

Substantial self-immolation of BBOT (**1**) occurred within 2–6 hours, supported by the shift of the benzylic peak from 5.43 to 3.91 (Fig. 2, B to B1). For BBOC (**3**), the benzylic proton peak had a relatively small upfield shift (δ 4.99 to 4.85 ppm, Scheme S2†), possibly due to a slower self-immolation of the resultant carbamate-phenol intermediate under the organic solvent conditions (Scheme S2, peak B†). Both reactions were

conducted in a mixture of organic : aqueous solvent (DMSO-d_6/D_2O-PBS, 4 : 1), which was expected to slow the rate of self-immolation compared to pure aqueous conditions.[41,42]

Based on our previous aryl azide self-immolative methacrylates activated by H_2S,[39] the quinone methide formed was expected to quench with phosphate or water;[39,42] however this was not observed for the arylboronate methacrylate BBOT (**1**). Instead, the NMR evidence pointed towards attack of the released alkyl amine on the electrophilic methide to afford amine-linked methacylate analogue **8** (Scheme 2 and Fig. 2). From the ^{1}H NMR study (Fig. 2), evidence suggesting the structure of **8** was provided by the upfield shift in the benzylic protons (B to B1; δ 5.44 to δ 3.92) and alkyl chain protons (C to C1; δ 4.20/3.69 to 4.06/3.38). If water or phosphate had reacted with the methide in place of the amine group, the benzylic protons at B/B1 would be expected to shift to δ ~4.35 ppm (4-hydroxybenzyl alcohol) and δ ~5 ppm (4-hydroxybenzyl phosphate);[39,42] absent peaks in the NMR spectrum for **1** (Fig. 2). Alternatively, H_2S generated from the released COS could itself act as a nucleophile and form a benzyl thiol compound (aromatic–CH_2–SH). However, there was no observed benzylic proton (CH_2) shift at δ ~3.92 ppm in our previous

report,[39] even though the methide was generated in a large excess of H_2S. This further supports the likely product with benzylic protons at 3.92 ppm as compound **8** and not a benzyl thiol.

The generation of COS from BBOT (**1**) *via* carbonic anhydrase (enzymatic) catalysed hydrolysis of COS to H_2S was detected by measuring the activation of pro-fluorophore 7-azido-4-methylcoumarin (AzMC)[43] (Fig. 3). BBOT (**1**), FBOT (**2**) and BBOC (**3**) were solubilised in PBS : DMSO (9 : 1) and incubated at 37 °C in the presence of H_2O_2 (10-fold excess) at pH 7.4. Activation of the pro-fluorophore AzMC was fast, with a rapid increase in fluorescence being observed when COS/H_2S-releasing BBOT (**1**) was incubated with H_2O_2 and CA (Fig. 3, red). The control polymers, non-triggerable FBOT (**2**) and triggerable but CO_2-releasing BBOC (**3**), produced no fluorescent signal (Fig. 3, green and blue). Further support for H_2S generation from BBOT (**1**) was provided by comparison to an equimolar amount of peroxyTCM-2, the control H_2O_2-responsive small molecule COS/H_2S donor[37] (Fig. 3, black). Compared to BBOT (**1**), peroxyTCM-2 (synthesis described in ESI, section 1.5†) produced a slightly faster increase in fluorescence output than BBOT (**1**). However, the fluorescent output was the same after approximately 6 hours incubation.

Block co-polymer (BCP) synthesis from methacrylates

The methacrylate monomers **1**, **2** and **3** were polymerised using Activators ReGenerated by Electron Transfer (ARGET) Atom Transfer Radical Polymerisation (ATRP).[39] ARGET-ATRP was selected for its relatively mild conditions so that the boronic ester and thiocarbamate bond would remain intact during polymerisation.[39] $mPEG_{2000}$ macroinitiator (calculated at 49 repeating units *via* NMR spectroscopic analysis) was used to initiate the reaction with sodium ascorbate as the reducing agent.[39,44] Targeted polymers of 10 kDa were synthesised to achieve a hydrophobic/hydrophilic balance of 0.2,[45] with consistent conversion and narrow polydispersity (Đ) (Table 1). BCPs containing the BBOT monomer (**1**) were isolated as $mPEG_{49}$-$BBOT_{24}$ (**10**, ~10 kDa, 24 × BBOT units, Đ = 1.19). The

control polymers, $mPEG_{49}$-$FBOT_{38}$ (**11**) and $mPEG_{49}$-$BBOC_{23}$ (**12**) were synthesized with similar molecular weights and Đ (Table 1). The relative integration of the benzylic protons to the PEG protons (Fig. S16, S18 and S21†) indicated that connection of methacrylate to the PEG unit had occurred without any undesired degradation of the capping group (including the thiocarbamate bond).

Formulation of polymers and H_2O_2 triggered activation of particles producing H_2S

Polymers were self-assembled *via* nanoprecipitation, using THF and the rapid addition of PBS. Compound vesicle-like particles[39] were generated (Fig. S4†) but these were unstable at 37 °C, with aggregation occurring and average measured particle size increasing over 8–24 hours (Fig. S5†). To increase steric stabilization, 9% w/w Pluronic F127 was added.[46,47] This prevented aggregation of the $mPEG_{49}$-$BBOT_{24}$ (**10**) particles (Fig. S5†) and resulted in particles of 130 ± 4 nm and narrow distribution (PDI = 0.106). Control polymers formed similar sized particles (Table S1†). The addition of Pluronic F127 altered particle morphology, giving a mixed morphology of polymersomes (vesicles) and large compound vesicles (Fig. 4A) with a unimodal particle size distribution of 130 ± 4 nm (Fig. 4C). The formation of these types of structures was in line with the increased time to kinetic entrapment.[39]

Oxidation of the arylboronate within the $mPEG_{49}$-$pBBOT_{24}$ (**10**) particles was achieved by exposure to 1 mM H_2O_2. Triggered activation of the $mPEG_{49}$-$BBOT_{24}$ particles (**10**) was explored using NMR, DLS, GPC, electron microscopy and fluorescence assays (Fig. 4).

For oxidation of the arylboronate to occur in the particles, H_2O_2 must partition into the hydrophobic bilayer. The time for diffusion is expected to influence the kinetics of COS production[20] which is expected to be slower than that of the free monomer.[31,42] As predicted, after incubating $mPEG_{49}$-$BBOT_{24}$ (**10**) with H_2O_2 (~10-fold excess), the generation of H_2S *via* conversion of COS was observed to increase slowly over 8 hours, with a maximal fluorescent output at 24 hours (Fig. 4E). This was slower than the triggering of BBOT (**1**) monomer and peroxyTCM-2 (seen in Fig. 3) and represented an approx. 3-fold increase in fluorescent signal output compared to the control particles **11** and **12** (Fig. 4E) which did not produce any COS/H_2S in the presence of H_2O_2 and carbonic anhydrase (background fluorescence only observed). While release was relatively slow for the $mPEG_{49}$-$BBOT_{10}$ particles, a challenge in H_2S delivery is the selective and controlled release of the gas.[12,13,20] The slower, steady H_2S profile shown in Fig. 4E could prove beneficial over more rapidly generating small molecule donors if the future application of the COS/H_2S donor particles is reinstating physiologically relevant concentrations of H_2S to mimic endogenous levels (instead of rapid bolus release).

^1H NMR spectroscopy was performed on recovered $mPEG_{49}$-$BBOT_{24}$ (**10**) particles (Fig. S6†). Exposure to control conditions (PBS only) resulted in no change to the ^1H NMR spectrum of $mPEG_{49}$-$BBOT_{24}$ (**10**) particles. Exposure to H_2O_2 reduced the
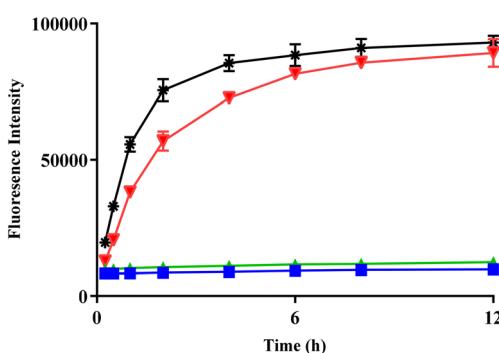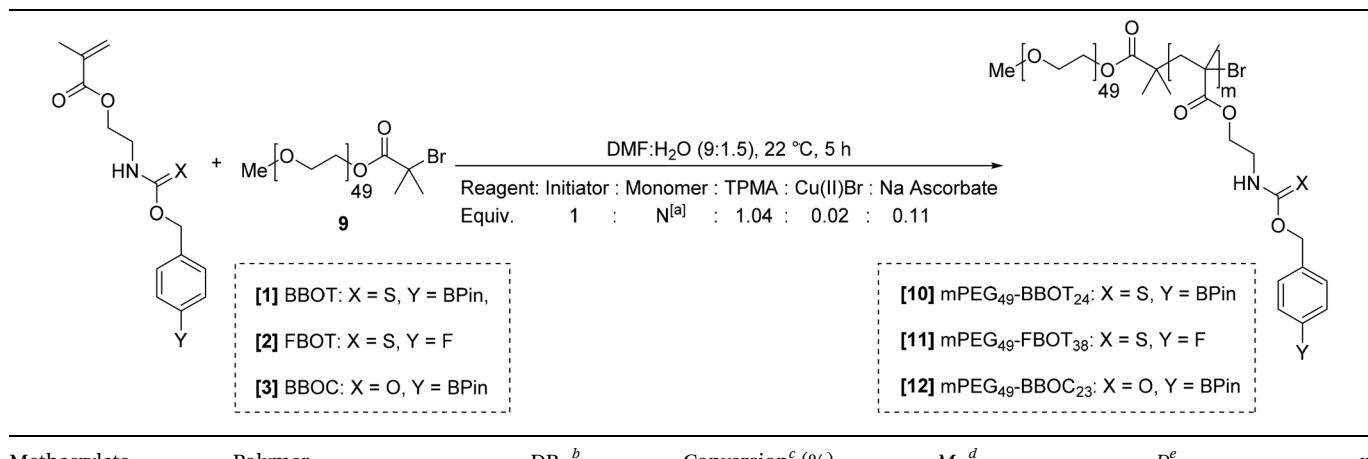

Fig. 3 Activation of pro-fluorophore 7-azido-4-methylcoumarin (AzMC) after exposure to H_2O_2 in the presence of carbonic anhydrase in PBS (pH 7.4) at 37 °C from peroxyTCM-2 (black), BBOT (**1**) (red), FBOT (**2**) (green) and BBOC (**3**) (blue), as measured by fluorescence ex/em: 355/460 nm.

© 2025 The Author(s). Published by the Royal Society of Chemistry

RSC Appl. Polym., 2025, **3**, 926–933 | **929**

Open Access Article. Published on 28 May 2025. Downloaded on 2/10/2026 5:35:33 PM.
This article is licensed under a Creative Commons Attribution-NonCommercial 3.0 Unported Licence.

Table 1 Characterisation of amphiphilic block-*co*-polymers synthesised *via* ARGET ATRP

Reagent: Initiator : Monomer : TPMA : Cu(II)Br : Na Ascorbate
Equiv.   1   :   N[a]   : 1.04 : 0.02 :   0.11

DMF:H₂O (9:1.5), 22 °C, 5 h

[1] BBOT: X = S, Y = BPin,
[2] FBOT: X = S, Y = F
[3] BBOC: X = O, Y = BPin

[10] mPEG₄₉-BBOT₂₄: X = S, Y = BPin
[11] mPEG₄₉-FBOT₃₈: X = S, Y = F
[12] mPEG₄₉-BBOC₂₃: X = O, Y = BPin

Methacrylate	Polymer	DP_n [b]	Conversion[c] (%)	M_n [d]	$Đ$ [e]	n
1	mPEG₄₉-BBOT₂₄ (**10**)	24	93 ± 3	11 859 ± 906	1.19 ± 0.03	8
2	mPEG₄₉-FBOT₃₈ (**11**)	38	94	13 643	1.17	1
3	mPEG₄₉-BBOC₂₃ (**12**)	23	79 ± 16	11 439 ± 627	1.30 ± 0.08	4

[a] Number of moles monomer/methacrylate used (**1**, **2**, or **3**) described in the ESI.† [b] Degree of polymerisation. [c] Conversion of monomers into polymer, determined from molar input and DP_n. [d] Number average molecular weight, determined *via* ¹H NMR analysis. [e] Determined *via* GPC analysis (M_w/M_n, see ESI†). n = replicate polymerisations. TPMA = tris(2-pyridylmethyl)amine.
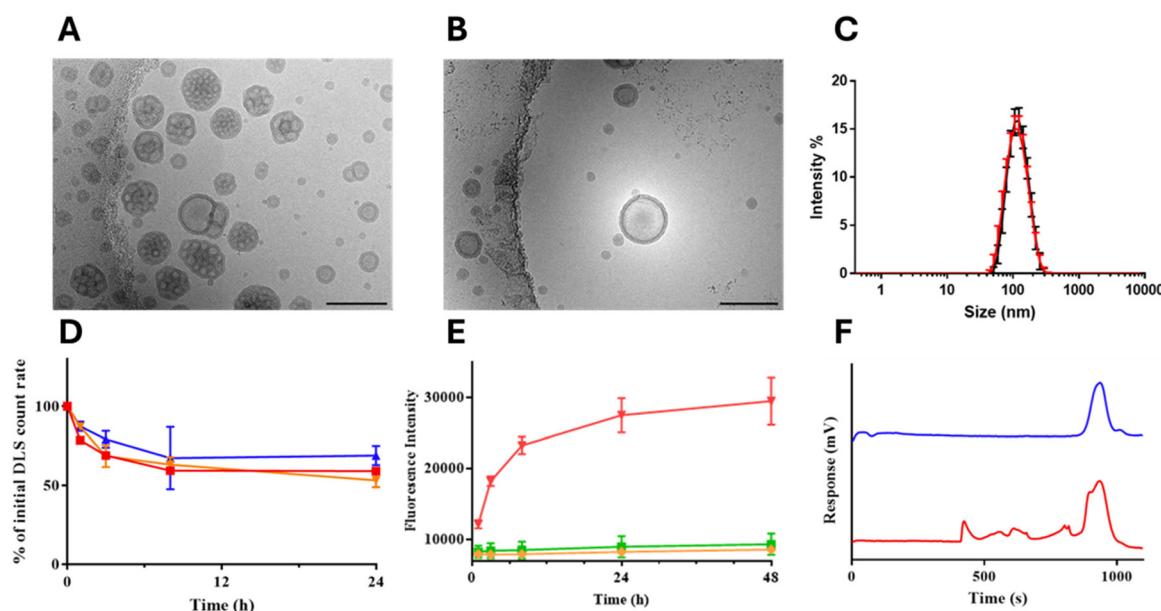

Fig. 4 Cryo-TEM of mPEG₄₉-pBBOT₂₄ particles (**10**) formulated with Pluronic F127 9% w/w prior to (A) and after (B) exposure to 1 mM H₂O₂. Scale bar is 200 nm. (C) DLS histogram of particles after exposure to PBS (control, black) or 1 mM H₂O₂ (red). (D) Remaining DLS derived count rate of particles after exposure to PBS control (blue), 0.1 mM (orange) or 1 mM (red) H₂O₂. (E) Activation of pro-fluorophore AzMC *via* H₂O₂-triggering (~10-fold excess) of mPEG₄₉-BBOT₂₄ (**10**, red), mPEG₄₉-BBOC₂₃ (**12**, green) or mPEG₄₉-FBOT₃₈ (**11**, blue) particles (all formulated with 9% w/w Pluronic and incubated with carbonic anhydrase), as measured by fluorescence ex/em: 355/460 nm. (F) GPC analysis of recovered polymers after exposure to PBS (blue) or 1 mM H₂O₂ (red) for 24 hours.

relative intensity of aromatic and benzylic protons (derived from methacrylate backbone) to the PEG backbone, suggesting that self-immolation had occurred with diffusion of these groups out of the bilayers and removal during dialysis.

Exposure of the control mPEG₄₉-FBOT₃₈ (**11**) particles to H₂O₂ showed no changes in the ¹H NMR spectrum (Fig. S7†).

Qualitative GPC was performed on control (PBS only) and triggered (H₂O₂) particles after lyophilization (Fig. 4F). The

polymers had an apparent increase in MW and polydispersity, suggesting extensive cross-linking had occurred within the bilayers, although no quantification was performed. The cross-linking resulted in stable particles that retained their initial morphology. DLS showed an unchanged particle size distribution (Fig. 4C) and particle counts for the triggered and non-triggered particles (Fig. 4D). This suggests particles do not lyse upon H_2O_2 exposure, similar to the non-triggerable control particles, mPEG$_{49}$-FBOT$_{38}$ (**11**) (Fig. S8†). Triggerable control mPEG$_{49}$-BBOC$_{23}$ (**12**) particles exhibited a rapid reduction in DLS count rates when exposed to H_2O_2 (Fig. S9†). Cryo-TEM (Fig. 4B) on H_2O_2 exposed mPEG$_{49}$-BBOT$_{24}$ (**10**) particles showed well-defined vesicles, but with a potential loss of the internal particle structures seen prior to H_2O_2 exposure (Fig. 4A). This suggests polymer cross-linking may occur when the primary amines within the bilayer are liberated[48,49] in the more non-polar bilayer of the thiocarbamate in mPEG$_{49}$-BBOT$_{24}$ (**10**), as compared to the carbamate mPEG$_{49}$-BBOC$_{23}$ (**12**) particles which underwent lysis.[39] The crosslinking *via* an amide bond-forming reaction was further supported by FTIR analysis (Fig. S10†), with a new amide carbonyl (C=O) bond stretch at 1654 cm^{-1}.[39]

Of note, the above studies were conducted in buffer with a single triggering agent (H_2O_2), but in a complex biological environment there may be other triggers that can lead to H_2S generation, such as cysteine, which has been shown to diffuse into micelles and release H_2S.[20] However, the location of the arylboronate/thiocarbamate group in the hydrophobic portion of the vesicle is expected to provide some protection, especially to more polar activators. The observed slower rate of H_2S-release for the mPEG$_{49}$-BBOT$_{24}$ (**10**) vesicles (Fig. 4E) compared to the monomer methacrylate BBOT (**1**) (Fig. 3) could also indicate that diffusion[20] of H_2O_2 is rate-determining in H_2S release from the vesicles.

Encapsulation of drug cargo in H_2S-producing particles

Finally, the COS/H_2S-producing nanoparticles were examined for their potential as a drug delivery system. Such a system could be used to deliver a dual payload (whereby a therapeutic effect is exerted by H_2S and cargo in a synergistic fashion[23,50]) or to limit off target toxicities.[28] To increase loading potential self-assembly was performed with 2 mg mL^{-1} polymer concentration, resulting in larger particles of 164 ± 8 nm when unloaded or 217 ± 4 nm when loaded (Tables S2 and S3†).

Self-assembled mPEG$_{49}$-BBOT$_{24}$ (**10**) particles were passively loaded with doxorubicin·HCl (Table S3†) and achieved a drug loading content of 2.3%.[30] Higher loading was achieved for the mPEG$_{49}$-BBOT$_{24}$ (**10**) > mPEG$_{49}$-BBOC$_{23}$ (**12**) > mPEG$_{49}$-FBOT$_{38}$ (**11**), which is speculated to be related to the relative hydrophilicities of the monomeric components ($C\log P$ 4.9, 4.2 and 3.5, respectively). Triggering with H_2O_2 resulted in release of the model drug (Fig. 5). As particles are not lysed (Fig. 4) this suggests bilayers become permeable to small molecules and provides evidence these systems could have a dual function.
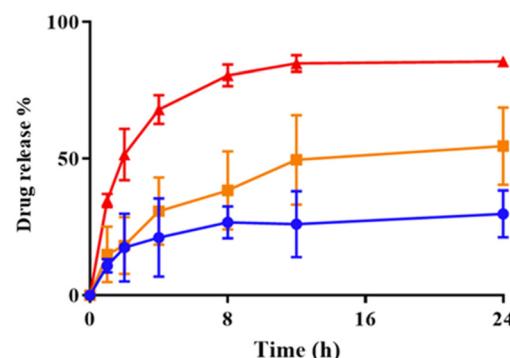

Fig. 5 Release of doxorubicin·HCl from mPEG$_{49}$-BBOT$_{24}$ (**10**) particles in response to PBS control conditions (blue), 0.1 mM (orange) or 1 mM (red) H_2O_2 at 37 °C. Mean ± SD, n = 3.

Conclusions

Polymeric nanoparticles containing caged carbonyl sulfide (COS) in the thiocarbamate bond of the polymer backbone were formulated from mPEGylated polymers. The thiocarbamate polymer backbone was functionalised with repeating arylboronate monomers that were synthesized *via* ARGET-ATRP. The polymer BBOT (**1**) and the polymeric nanoparticles mPEG$_{49}$-BBOT$_{24}$ (**10**) were oxidised by H_2O_2, activating the release of COS and generation of H_2S *via* carbonic anhydrase hydrolysis. The released H_2S caused a reduction of the azide group in pro-fluorophore AzMC and a measurable fluorescent output. The control, non-COS/H_2S generating monomers FBOT (**2**) and BBOC (**3**), and the mPEG$_{24}$-FBOT$_{38}$ (**11**)/mPEG$_{49}$-BBOC$_{23}$ (**12**) nanoparticles did not reduce/activate the pro-fluorophore AzMC, providing a strong case for future *in vivo* work using the mPEG$_{49}$-BBOT$_{24}$ (**10**) particles for azido-prodrug activation strategies.

Overall, these larger donors complement the current arsenal of small molecule H_2S donors and could have therapeutic potential in diseases with low levels of H_2S or provide a targeted method for aryl azide reduction and activation of pro-drugs and drug release.

Author contributions

D. A. P. designed and conducted most of the experiments, supervised J. D., and contributed to project ideas. A. L. contributed to the design and synthesis and provided expertise in synthetic chemistry. J. D. conducted some of the synthesis and formulation experiments with D. A. P. S. H. provided supervision and guidance on the formulation of nanoparticles and contributed to project ideas. A. B. G. conceived the project idea and provided overall supervision of the project and experiments. D. A. P. and A. B. G. wrote the manuscript with contributions to the final version from all the authors.

© 2025 The Author(s). Published by the Royal Society of Chemistry

RSC Appl. Polym., 2025, **3**, 926–933 | 931

Data availability

The data, including complete experimental methods, supporting this article have been included as part of the ESI.† The following additional references can be found in the ESI.† [51,52]

Conflicts of interest

There are no conflicts to declare.

Acknowledgements

References

1 R. Wang, *FASEB J.*, 2002, **16**, 1792–1798.

2 J. L. Wallace and R. Wang, *Nat. Rev. Drug Discovery*, 2015, **14**, 329–345.

3 M. D. Hartle and M. D. Pluth, *Chem. Soc. Rev.*, 2016, **45**, 6108–6117.

4 J. Bełtowski, *Pharmacol. Rep.*, 2015, **67**, 647–658.

5 H. Zhu, V. Dronamraju, W. Xie and S. S. More, *Med. Chem. Res.*, 2021, **30**, 305–352.

6 Y. Chen, F. Zhang, J. Yin, S. Wu and X. Zhou, *J. Cell Physiol.*, 2020, **235**, 9059–9070.

7 Y.-Z. Wang, E. E. Ngowi, D. Wang, H.-W. Qi, M.-R. Jing, Y.-X. Zhang, C.-B. Cai, Q.-L. He, S. Khattak, N. H. Khan, Q.-Y. Jiang, X.-Y. Ji and D.-D. Wu, *Int. J. Mol. Sci.*, 2021, **22**, 2194.

8 B. Liu, S. Wang, M. Xu, Y. Ma, R. Sun, H. Ding and L. Li, *Front. Pharmacol.*, 2022, **13**, 899859.

9 Z.-L. Song, L. Zhao, T. Ma, A. Osama, T. Shen, Y. He and J. Fang, *Med. Res. Rev.*, 2022, **42**, 1930–1977.

10 C. Szabo, C. Coletta, C. Chao, K. Módis, B. Szczesny, A. Papapetropoulos and M. R. Hellmich, *Proc. Natl. Acad. Sci. U. S. A.*, 2013, **110**, 12474–12479.

11 C. Munteanu, M. A. Turnea and M. Rotariu, *Antioxidants*, 2023, **12**, 1737.

12 H. Lu, Y. Chen and P. Hu, *Adv. Ther.*, 2023, **6**, 2200349.

13 Y. Zheng, B. Yu, L. K. De La Cruz, M. R. Choudhury, A. Anifowose and B. Wang, *Med. Res. Rev.*, 2018, **38**, 57–100.

14 B. Szczesny, K. Módis, K. Yanagi, C. Coletta, S. Le Trionnaire, A. Perry, M. E. Wood, M. Whiteman and C. Szabo, *Nitric Oxide*, 2014, **41**, 120–130.

15 E. E. Ngowi, A. Afzal, M. Sarfraz, S. Khattak, S. U. Zaman, N. H. Khan, T. Li, Q.-Y. Jiang, X. Zhang, S.-F. Duan, X.-Y. Ji and D.-D. Wu, *Int. J. Biol. Sci.*, 2021, **17**, 73–88.

16 E. R. DeLeon, G. F. Stoy and K. R. Olson, *Anal. Biochem.*, 2012, **421**, 203–207.

17 M. C. Urquhart, N. V. Dao, F. Ercole, B. J. Boyd, T. P. Davis, M. R. Whittaker and J. F. Quinn, *ACS Macro Lett.*, 2020, **9**, 553–557.

18 C. R. Powell, J. C. Foster, S. N. Swilley, K. Kaur, S. J. Scannelli, D. Troya and J. B. Matson, *Polym. Chem.*, 2019, **10**, 2991–2995.

19 K. Kaur, R. J. Carrazzone and J. B. Matson, *Antioxid. Redox Signal.*, 2019, **32**, 79–95.

20 J. C. Foster, R. J. Carrazzone, N. J. Spear, S. C. Radzinski, K. J. Arrington and J. B. Matson, *Macromolecules*, 2019, **52**, 1104–1111.

21 S.-S. Qi, J.-H. Sun, H.-H. Yu and S.-Q. Yu, *Drug Delivery*, 2017, **24**, 1909–1926.

22 Y. S. Loo, N. I. Zahid, T. Madheswaran and I. D. M. Azmi, *J. Drug Delivery Sci. Technol.*, 2022, **71**, 103300.

23 J. C. Foster, S. C. Radzinski, X. Zou, C. V. Finkielstein and J. B. Matson, *Mol. Pharm.*, 2017, **14**, 1300–1306.

24 N. V. Dao, F. Ercole, L. M. Kaminskas, T. P. Davis, E. K. Sloan, M. R. Whittaker and J. F. Quinn, *Biomacromolecules*, 2020, **21**, 5292–5305.

25 S. H. Yu, L. Esser, S. Y. Khor, D. Senyschyn, N. A. Veldhuis, M. R. Whittaker, F. Ercole, T. P. Davis and J. F. Quinn, *J. Polym. Sci., Part A: Polym. Chem.*, 2019, **57**, 1982–1993.

26 X. Dong, R. K. Brahma, C. Fang and S. Q. Yao, *Chem. Sci.*, 2022, **13**, 4239–4269.

27 A. Xie, S. Hanif, J. Ouyang, Z. Tang, N. Kong, N. Y. Kim, B. Qi, D. Patel, B. Shi and W. Tao, *EBioMedicine*, 2020, **56**, 102821.

28 K. M. Dillon, R. J. Carrazzone, Y. Wang, C. R. Powell and J. B. Matson, *ACS Macro Lett.*, 2020, **9**, 606–612.

29 N. Ma, Y. Li, H. Ren, H. Xu, Z. Li and X. Zhang, *Polym. Chem.*, 2010, **1**, 1609–1614.

30 E. Jäger, O. Ilina, Y. Dölen, M. Valente, E. A. W. van Dinther, A. Jäger, C. G. Figdor and M. Verdoes, *Biomacromolecules*, 2024, **25**, 1749–1758.

31 K. E. Broaders, S. Grandhe and J. M. J. Fréchet, *J. Am. Chem. Soc.*, 2011, **133**, 756–758.

32 C. R. Powell, K. M. Dillon and J. B. Matson, *Biochem. Pharmacol.*, 2018, **149**, 110–123.

33 C. M. Levin, M. M. Cerda and M. D. Pluth, *Acc. Chem. Res.*, 2019, **52**, 2723–2731.

34 C. M. Levin, A. K. Steiger and M. D. Pluth, *ACS Chem. Biol.*, 2019, **14**, 170–175.

35 A. K. Steiger, S. Pardue, C. G. Kevil and M. D. Pluth, *J. Am. Chem. Soc.*, 2016, **138**, 7256–7259.

36 C. M. Levin, M. M. Cerda and M. D. Pluth, *Antioxid. Redox Signal.*, 2019, **32**, 96–109.

37 Y. Zhao and M. D. Pluth, *Angew. Chem., Int. Ed.*, 2016, **55**, 14638–14642.

38 C. Li, J. Hu, T. Liu and S. Liu, *Macromolecules*, 2011, **44**, 429–431.

39 D. A. Paterson, W.-K. Fong, S. Hook and A. B. Gamble, *Biomacromolecules*, 2021, **22**, 4770–4782.

40 A. K. Steiger, M. Marcatti, C. Szabo, B. Szczesny and M. D. Pluth, *ACS Chem. Biol.*, 2017, **12**, 2117–2123.

41 J. S. Robbins, K. M. Schmid and S. T. Phillips, *J. Org. Chem.*, 2013, **78**, 3159–3169.

42 E. A. Garcia, D. Pessoa and M. Herrera-Alonso, *Soft Matter*, 2020, **16**, 2473–2479.

43 M. K. Thorson, T. Majtan, J. P. Kraus and A. M. Barrios, *Angew. Chem., Int. Ed.*, 2013, **52**, 4641–4644.

44 K. Min, H. Gao and K. Matyjaszewski, *Macromolecules*, 2007, **40**, 1789–1791.

45 Y. Mai and A. Eisenberg, *Chem. Soc. Rev.*, 2012, **41**, 5969–5985.

46 J. Y. T. Chong, X. Mulet, L. J. Waddington, B. J. Boyd and C. J. Drummond, *Soft Matter*, 2011, **7**, 4768–4777.

47 J. Zhai, R. B. Luwor, N. Ahmed, R. Escalona, F. H. Tan, C. Fong, J. Ratcliffe, J. A. Scoble, C. J. Drummond and N. Tran, *ACS Appl. Mater. Interfaces*, 2018, **10**, 25174–25185.

48 Z. Deng, Y. Qian, Y. Yu, G. Liu, J. Hu, G. Zhang and S. Liu, *J. Am. Chem. Soc.*, 2016, **138**, 10452–10466.

49 X. Wang, G. Liu, J. Hu, G. Zhang and S. Liu, *Angew. Chem., Int. Ed.*, 2014, **53**, 3138–3142.

50 K. Chegaev, B. Rolando, D. Cortese, E. Gazzano, I. Buondonno, L. Lazzarato, M. Fanelli, C. M. Hattinger, M. Serra, C. Riganti, R. Fruttero, D. Ghigo and A. Gasco, *J. Med. Chem.*, 2016, **59**, 4881–4889.

51 R. Glaser, R. Hillebrand, W. Wycoff, C. Camasta and K. S. Gates, *J. Org. Chem.*, 2015, **80**, 4360–4369.

52 S. Modi and B. D. Anderson, *Mol. Pharm.*, 2013, **10**, 3076–3089.

© 2025 The Author(s). Published by the Royal Society of Chemistry

RSC Appl. Polym., 2025, **3**, 926–933 | **933**